



Published in final edited form as:

Genes Immun. 2019 July ; 20(6): 473–483. doi:10.1038/s41435-018-0040-1.

Fine-mapping Analysis of a Chromosome 2 Region Linked to Resistance to *Mycobacterium tuberculosis* Infection in Uganda Reveals Potential Regulatory Variants

Robert P. Igo Jr.¹, Noémi B. Hall¹, LaShaunda L. Malone², Jacob B. Hall^{1,3}, Barbara Truitt¹, Feiyou Qiu¹, Li Tao⁴, Ezekiel Mupere^{1,5,6}, Audrey Schnell¹, Thomas R. Hawn⁷, William S. Bush¹, Moses Joloba⁸, W. Henry Boom^{2,5}, Catherine M. Stein^{1,2,5,*}

¹Department of Population & Quantitative Health Sciences, Case Western Reserve University, Cleveland, OH USA ²Tuberculosis Research Unit (TBRU), Case Western Reserve University, Cleveland, OH USA ⁴Department of Internal Medicine, Harbor-UCLA Medical Center, Los Angeles, CA USA ⁵Uganda-Case Western Reserve University Research Collaboration, Kampala, Uganda ⁶Departments of Pediatrics & Child Health, and Medicine, School of Medicine, Makerere University and Mulago Hospital, Kampala, Uganda ⁷Department of Medicine, University of Washington, Seattle, WA ⁸School for Biomedical Sciences, College of Health Sciences, Makerere University, Kampala, Uganda

Abstract

Tuberculosis (TB) is a major public health burden worldwide, and more effective treatment is sorely needed. Consequently, uncovering causes of resistance to *Mycobacterium tuberculosis* (*Mtb*) infection is of special importance for vaccine design. Resistance to *Mtb* infection can be defined by a persistently negative tuberculin skin test (PTST–) despite living in close and sustained exposure to an active TB case. While susceptibility to *Mtb* is, in part, genetically determined, relatively little work has been done to uncover genetic factors underlying resistance to *Mtb* infection. We examined a region on chromosome 2q previously implicated in our genomewide linkage scan by a targeted, high-density association scan for genetic variants enhancing PTST– in two independent Ugandan TB household cohorts ($n = 747$ and 471). We found association with SNPs in neighboring genes *ZEB2* and *GTDC1* (peak meta $p = 1.9 \times 10^{-5}$) supported by both samples. Bioinformatic analysis suggests these variants may affect PTST– by regulating the histone deacetylase (HDAC) pathway, supporting previous results from transcriptomic analyses. An apparent protective effect PTST– against body-mass wasting suggests

Users may view, print, copy, and download text and data-mine the content in such documents, for the purposes of academic research, subject always to the full Conditions of use: http://www.nature.com/authors/editorial_policies/license.html#terms

*Address correspondence to: Catherine M. Stein, Ph.D., cmj7@case.edu, 216-368-5631.

³Current affiliation: Institute for Next Generation Healthcare, Icahn School of Medicine at Mount Sinai, New York, NY

Conflict of Interest

The authors declare that they have no conflict of interest.

Author Contributions

EM, MJ, WHB and CMS conceived and designed the study. EM and MJ recruited families and collected the study sample. LLM maintained the database of clinical study data. RPI, NHB, BT, FQ, LT and AS processed the raw genotype data and conducted quality control. TRH, WHB, and CMS developed the conceptual biologic model. RPI, NHB, JBH and WSB performed statistical analyses. RPI and CMS drafted the manuscript. All authors read and approved the final manuscript.

a link between resistance to *Mtb* infection and healthy body composition. Our results provide insight into how humans may escape latent *Mtb* infection despite heavy exposure.

Keywords

tuberculosis; genetic association; early clearance of *Mycobacterium tuberculosis*; genetics of immunity

Introduction

Tuberculosis (TB) is one of the most devastating communicable diseases in world health, with approximately 10.4 million incident cases and 1.4 million deaths from TB in 2015¹. About nine in ten people initially infected with *Mycobacterium tuberculosis* (*Mtb*), however, do not go on to develop active disease. Hence, TB pathogenesis follows a two-step process², starting with initial infection, (latent *Mtb* infection, LTBI) diagnosed by the tuberculin skin test (TST) or interferon-gamma release assays (IGRA), and progression to symptomatic disease in a subset of infected persons.

While a role for human genetic susceptibility to TB has been well-established^{3, 4}, genetic susceptibility to *Mtb* infection has been less studied. Genomewide analyses of TB, whether for genetic linkage^{5–9} or, more recently, for association^{10–17}, have not provided consistent evidence for major TB susceptibility loci. Difficulty of replication may stem in part from the clinical definitions used for TB¹⁸. Few studies have examined latent *Mtb* infection^{7, 17, 19–21}; yet, while few, these studies reveal consistency in genomic loci identified.

Within the framework of household contact study^{22, 23}, we have focused on the persistent TST negative (PTST–) phenotype, which measures relative resistance to *Mtb* infection over an extended period of time, despite heavy exposure within the household²⁴. The hypothesis that this resistance may be influenced by innate and adaptive immune factors is an ongoing area of investigation^{25–27}. Studying resistance may reveal genetic insights into mechanisms underlying TB pathogenesis^{16, 21}. Resistance to latent *Mtb* infection has particular relevance to the design of a preinfection vaccine²⁶, since reducing the pool of latently infected individuals will reduce the incidence of TB. Analysis of PTST– individuals could identify critical biologic mechanisms underlying resistance to *Mtb* infection.

We previously found evidence for genetic linkage of regions on chromosome 2q and 5p with the PTST– phenotype⁷. We then found genetic association with the PTST– phenotype at an existing candidate locus, SLC6A3, within the chromosome 5 region²⁸ that had been identified by another group examining TST reactivity^{17, 19, 20}. Now, we present a fine-mapping association scan for PTST– across the other major linkage region, on chromosome 2q, with two independent samples from Ugandan households ascertained through an index case with TB^{22, 23, 29}. Heritability analysis suggested that approximately half of the genetic variation in PTST– is due to loci on chromosome 2q. A meta-analysis combining the two samples identified two loci of interest, one linked to histone de-acetylase regulation, and

another linked to body mass composition, uncovering new biologic pathways underlying resistance to *Mtb* infection.

Results

Sample Description

Our study sample comprises two independently-recruited cohorts of Ugandan households ascertained through a proband with active TB (summarized in Table 1)^{22, 29}. Sample 1 ($n = 165$ active TB, 501 LTBI, 81 PTST-) was genotyped for a fine-mapping panel with markers spaced approximately every 10 kb across the chromosome 2 linkage peak observed in an overlapping sample (overlap $n = 103$ TB, 277 LTBI and 45 PTST-)⁷, and subsequently imputed to the Illumina HumanOmni5 panel. In addition, genotyping for haplotype tagging SNPs from several candidate loci that may affect resistance to *Mtb* infection²⁸ was performed. Sample 2 ($n = 201$ TB, 237 LTBI, 33 PTST-), genotyped for the Illumina HumanOmni5 BeadChip (average marker distance ~ 600 bp), includes a greater proportion of participants with active TB and a smaller proportion of PTST-. In both samples, PTST- are, on average, much younger than non-PTST-, but did not differ significantly in sex ratio or in proportion of HIV+ individuals.

Genetic Association Analysis

We focused on SNPs that showed association in both samples, thus demonstrating internal replication. We tested genetic association in both samples by means of logistic regression, with adjustment for relatedness, and combined results for markers tested in both cohorts, after correction for population structure by genomic control (Supplementary Figure 1; see Supplementary Table 1 for complete results; the most significantly associated SNPs within each sample are listed in Supplementary Tables 2 and 3).

ZEB2/GTDC1 association peaks—The leading combined association result, for rs7568133 (145.2 Mb; $OR_{meta} = 2.12$, 95% CI = (1.50, 3.00) for the A allele; $p = 1.9 \times 10^{-5}$; Figure 1A, Table 2), follows from nominally significant associations in both study samples ($p = 0.00062$ and 0.0085 in Samples 1 and 2, respectively) (Table 2; Figures 1 and 2). The effect of this variant is consistent between Samples 1 ($OR = 2.00$, 95% CI = [1.35, 2.98]) and 2 ($OR = 2.54$, 95% CI = [1.27, 5.11]; p value from Cochran's Q test for heterogeneity = 0.56), and the minor allele frequencies are similar (0.495 vs. 0.478 in Samples 1 and 2, respectively). rs7568133 falls within the large intron 2 of the DNA-binding transcriptional repressor gene, zinc finger E-box-binding homeobox 2 (*ZEB2*; Figure 2A). This variant alters several potential DNA-binding motifs, and is an enhancer mark in primary monocytes, but is not listed as an expression quantitative trait locus (eQTL) in the GTEx database (Supplementary Table 4).

The overall region of association at *ZEB2* is primarily driven by strong associations in Sample 1 (Figure 2B), and extends about 200 kb to overlap with the glycosyltransferase-like domain-containing 1 (*GTDC1*) gene (Figure 2). Three markers within the association peak are among the five most significantly associated markers for Sample 1 (Supplementary Table 2). Of these, rs13390689 and rs79319398 are in introns: *GTDC1* intron 3 and *ZEB2* intron

2, respectively. Of particular interest is rs79319398, which lies within a DNA region associated with numerous enhancer histone-modification sites in monocytes, neutrophils, and B- and T-lymphocytes, and is predicted to affect three regulatory motifs (Supplementary Table 4). This variant also has a CADD score of 14.59, placing it in the top 3.5% of all possible genetic variants for deleteriousness. Though not within a gene, rs7580080, 7.8 kb downstream of *ZEB2*, is also connected in epigenomic studies to histone modification marks in monocytes, neutrophils and hematopoietic stem cells, and has a CADD score of 17.66 (Supplementary Table 4).

The association peaks in *ZEB2* and *GTDC1* appear to be independent. Associated variants in this region (Figure 2B, marked with asterisks) mostly lie within a single LD block within *GTDC1* (Supplementary Figure 2); however, rs7568133, is independent of this block and in only weak LD with one other associated SNP in *ZEB2*, rs79319398. A conditional association analysis of variants in the *GTDC1/ZEB2* region, in which allele dosages of rs7568133 were included as a covariate, confirmed the independence of this SNP from the associated SNPs in *GTDC1*, in that adjusting for the rs7568133 genotype did not reduce the significance of association of the *GTDC1* markers by more than an order of magnitude (data not shown). Haplotypes of the 11 SNPs in the LD block, which are highly correlated (r^2 near 1.0), and of two SNPs in *ZEB2*, rs7568133 and rs79319398, which are in complete LD ($D' = 1$) but not strongly correlated (Supplementary Figure 2), were tested for association with PTST- in Samples 1 and 2, but were not found to be more significantly associated than the best single markers (data not shown).

Because HIV status is a potential confounder for TST results, we conducted a sensitivity analysis in which HIV+ individuals were omitted. Although the p values for some of the highly associated SNPs in Table 2 were slightly less significant, most likely on account of the smaller number of available individuals, the ORs were very similar (data not shown), indicating that HIV status is not a major cause of misclassification.

FMNL2/ARL6IP6 association peak—In addition, several SNPs in ADP ribosylation factor-like 6 interacting protein 6 (*ARL6IP6*) were associated in both samples and had meta p -values $< 3 \times 10^{-5}$ (Table 2), although evidence of association was stronger from Sample 2 (Supplementary Table 3). However, the CADD scores for these SNPs were not notable, and none of them was listed in the GTEx database as an eQTL (Phred-scaled score < 3 ; Supplementary Table 4). Because the SNPs were not potentially pathogenic, and also because this gene did not have a potential connection to *Mtb* biology, it was not considered further as a candidate gene. Other strongly associated markers ($p < 10^{-4}$) from the meta-analysis have greatest support from Sample 2 (Table 2). Only one, rs58110523, is within a gene (intronic to *FMNL2* $p < 0.01$ in both individual samples), but resides in a region with very little association in Sample 1 (Figure 1). These variants, like the index variant rs7568133, change multiple binding motifs but are not linked to many epigenetic marks or transcription factor binding sites (Supplementary Table 4).

Regional heritability analysis

From our variance components analysis for region-specific heritability, we estimated that the chromosome 2 linkage interval explains 9.22% of PTST– risk in Sample 2 (SE = 5.59%; one-sided $p = 0.044$). The remainder of the autosomal genome explains 12.5% of the overall risk (SE = 6.17%; one-sided $p = 0.0084$); thus, the whole genome accounts for 21.7% of the risk.

Body mass composition

Because body-mass wasting is correlated to *Mtb* infection susceptibility^{30–34}, and because *GTDC1* has been associated with obesity-related phenotypes in a previous genomewide methylation scan³⁵, we examined the relationship between body mass parameters and PTST– status in our cohort. A smaller proportion of PTST– participants displayed evidence of body-mass wasting than non-PTST– participants by all three measured criteria: BMI, lean mass and fat mass (Table 3). However, only the lean-mass measurement showed a statistically significant difference (5.1% of PTST–s vs. 17.9% of non-PTST–s; $p = 0.039$). The non-PTST– subjects have a higher prevalence of lean-mass wasting than the PTST– subjects.

Discussion

We conducted a fine-mapping study exploring genetic variation associated with the PTST– phenotype in two Ugandan household samples over a segment of chromosome 2q with previous evidence for genetic linkage⁷. We measured disproportionate overall heritability attributable to the region, and more specifically, associated markers in both cohorts and through meta-analysis with the PTST– phenotype. Even though the risk for PTST– attributable to the chromosome 2 linkage region was only borderline significant ($p = 0.044$), this 51-Mb segment accounted for approximately 9% of the overall risk for, PTST– and more than 40% of the total genomic risk. These results support the hypothesis that at least one major locus underlying PTST– lies in this chromosomal region.

The most significant association result from the meta-analysis, rs7568133, implicates the genes *ZEB2* and *GTDC1* on 2q22.3. Though this result falls just short of regionwide significance (ca. 8×10^{-6}), this marker is associated in both samples with $p < 0.01$ and has good agreement in effect size. rs7568133 alters five potential regulatory motifs, and thus, although it is not upstream of either gene, it may function in regulation of gene expression. *ZEB2* contains a binding motif that potentially disrupts histone deacetylase 2 (*HDAC2*)³⁶, a gene implicated by gene-set enrichment analysis of differences in transcriptional response to *Mtb* infection by monocyte-derived macrophages from PTST– and non-PTST– individuals³⁷. The macrophage has a central role in *Mtb* pathogenesis, from recognition to killing, a key component of the innate immune response thought to influence PTST–^{25–27}. Thus, our results suggest that genetic variation in macrophage response may influence resistance to *Mtb* infection. Several SNPs with strong association in Sample 1 occur within enhancer histone marks and DNaseI-hypersensitivity sites found in numerous types of immune-system cells, implying that *ZEB2* may be under active transcription in these cell types. Moreover, three of these variants have CADD scores greater than 14 (Supplementary

Table 1), suggesting that these variants may truly be pathogenic. Together, these findings support a role for the HDAC innate immunity pathway in relative resistance to *Mtb* infection that may be genetically regulated.

The nearby gene, *GTDC1*, is involved with obesity and lipid metabolism. This gene may be of interest for TB pathology because resistance to *Mtb* infection is correlated with maintenance of body weight. Several previous studies reported that body mass composition is both a risk factor for development of active TB as well as for the speed of recovery from active TB^{30–34}. Here, we examined for the first time whether body composition was associated with resistance to *Mtb* infection. Body composition results (Table 3) show a significant decrease in lean mass body-mass wasting in PTST– vs. non-PTST–, despite the modest sample size. This leads to the hypothesis that *GTDC1* is a risk locus for lean mass wasting which in turn influences risk for *Mtb* infection. The ideal way to explore such a hypothesis is through Mendelian randomization analysis, which we are unable to perform in this dataset because there is not good overlap in the data with individuals having both genotype and bioelectrical impedance data. This will be the subject of future research. Hypocholesterolemia, a consequence of body-mass wasting, may increase susceptibility to *Mtb* infection through reduced activity of macrophages³⁸. Moreover, previous studies in mice suggest that hypercholesterolemia, whether induced by a high-cholesterol diet or by knockout of apolipoprotein E (*ApoE*), impairs the immune response to *Mtb* infection, with much greater susceptibility in *ApoE*^{–/–} mice^{39, 40}. In contrast, hypercholesterolemic mice lacking *LDL-R* did mount a robust immune response to *Mtb*, although, like the *ApoE*^{–/–} mice, the inflammatory response to *Mtb* was destructively exaggerated^{40, 41}, and statin drugs appear to increase resistance of human macrophages to *Mtb* infection⁴². Finally, methylation of *GTDC1* was found to be associated with waist circumference in a European American cohort, but the result was not successfully replicated³⁵.

The chromosome 2 region featured in the present study has also been recently replicated in its association with *Mtb* infection in a cohort of HIV-infected individuals²¹. There, a different extreme phenotype approach was taken, by focusing on individuals that were especially susceptible to *Mtb* infection because they were immunosuppressed and living in TB-endemic settings. In addition, the associated SNPs from this analysis explained the original linkage result. This, in combination with our region-specific heritability estimate, provides evidence for at least one associated locus in this region. rs7568133 is 14 Mb from the major 2q linkage peak for the PTST– phenotype reported earlier⁷, with greatest LOD score at microsatellite marker ATA27H09 (D2S1353, 2q24.1 at chr2:159,558,931–159,559,082), and a secondary LOD score peak at GATA4E11 (D2S410, 2q14.1 at chr2:116,240,929–116,241,085). Six of the eight most significantly associated markers from the meta-analysis are within 10 Mb of ATA27H09, suggesting that the linkage signal was not caused by a single genetic variant of large effect.

This investigation has several limitations and strengths. First, the power is restricted by the number of available PTST– individuals. Family relationships within the sample reduce the number of effective independent individuals and family-based association requires a more complex association test. Together, these constraints prevent detection of causal variants with uncommon alleles (frequency < 0.05) unless they are of large (quasi-Mendelian) effect.

Next, the use of Sample 2 HumanOmni5 genotypes as a reference for imputation of Sample 1 untyped variants potentially compromises the independence of the two samples. However, the differences in the major results from the individual samples (Supplementary Table 1; Supplementary Table 2) suggests that the induced correlation, if any, was slight. Our earlier report²³ shows a difference between level of exposure to TB index cases and PTST- vs. LTBI; however, this association is limited to children aged 5 to 15. Finally, the study samples are different in two respects: the average age for both PTST- and non-PTST- individuals is greater in Sample 2, and more non-PTST- have active TB in the Sample 2. These limitations attributable to small sample size are partly due to the observational nature of the study, whereby some subjects were lost to follow-up prior to the end of the 2-year observation period, therefore excluding them from analysis.

In conclusion, we observed an association between PTST- and *ZEB2*, further supporting a role for differential regulation of the HDAC pathway in individuals resistant to *Mtb* infection. These variants are likely functional based on high CADD score and presence of enhancer histone marks. Evidence for *GTDC1* was weaker, but further suggests a role for body composition in differential trajectories in TB pathogenesis. Deep resequencing, replication, and functional studies are needed to clarify the roles of these genes in *Mtb* infection.

Materials and methods

Study samples and phenotypes

All procedures performed in studies involving human participants were in accordance with the principles of the Declaration of Helsinki. All study protocols were reviewed and approved by the National HIV/AIDS Research Committee, the Uganda National Council of Science and Technology, and the institutional review board at the University Hospitals Case Medical Center, Cleveland, OH, USA. Informed consent was obtained from all participants.

Participants in Sample 1, the initial sample for fine mapping, were recruited as reported previously^{7, 23, 28}. Briefly, index cases with culture-positive pulmonary TB and their household members were enrolled and evaluated for TB symptoms and reactivity to TST. Participants were classified as PTST- if they tested TST- at recruitment and remained TST- over 24 months of follow-up. Because the TSTs were at least 3 months apart, boosting was unlikely to increase the chances of observing a TST conversion, as we demonstrate elsewhere²³. The sample after quality control totalled 747 individuals with a PTST- phenotype²⁸. This sample overlapped with the sample previously studied by linkage analysis⁷: 360 individuals belonged to both samples.

Individuals in Sample 2, the follow-up sample, were recruited later in the same study, but are independent from Sample 1. A total of 471 individuals from Sample 2 passed quality controls (see below).

HIV-negative individuals at least 15 years of age were measured for body-mass wasting by three related measures: body-mass index (BMI) and its two components, fat mass index (FMI) and lean mass index (LMI)⁴³. The overall sample for body-mass composition

comprised 232 PTST– and 1553 non-PTST– individuals from the household contact study^{22, 23}, including 236 individuals genotyped in Sample 1 (41 PTST–, 195 non-) and 253 individuals in Sample 2 (23 PTST–, 230 non-). Not all individuals had available measurements for all three measures. FMI and LMI were estimated by means of bioelectrical impedance analysis³⁰. Criteria for wasting were body-mass index (BMI) < 18.5 kg/m², fat mass index < 1.8 kg/m² for men and < 3.9 kg/m² for women, and lean mass index < 16.7 kg/m² for men and < 14.6 kg/m² for women³⁰.

The datasets analyzed in the current study are not publicly available, because the Ugandan participants did not consent to broad data sharing. However, individual-level data may be requested through a data access committee, chaired by Dr. Sudha Iyengar (ski@case.edu). All genetic association results (summary statistics) are available in Supplementary Table 1 (Online Resource 2).

Genotypes and quality control (QC)

The first phase of the study, conducted on Sample 1, focused on fine mapping a genomic region previously implicated by linkage analysis, 146–176 Kosambi cM on chromosome 2q⁷. We selected single-nucleotide polymorphisms (SNPs) within map position range chr2: 116,623,530–170,141,754, in GRCh37 coordinates, to cover the 1-LOD support interval (an approximate 95% confidence interval for location) underneath the linkage peak for the PTST– phenotype, at approximately 10-kilobasepair (kb) intervals for genotyping by means of the Illumina (San Diego, CA) iSelect platform. One informative SNP (minor allele frequency (MAF) = 0.1) was selected within each 10-kb window with maximum Illumina assay design score. Of 4,672 SNPs attempted, 3,626 were successfully genotyped on Sample 1 and processed using Illumina Genome Studio, and 3,478 passed marker QC (call rate = 0.9, minor allele frequency = 0.005, $p > 10^{-6}$ from exact test of deviation from Hardy-Weinberg proportions (HWP) in unrelated subjects, as tested by PLINK⁴⁴). Sample QC for the primary analysis has been described²⁸. Samples with call rate < 0.95 over the fine-mapping panel were omitted (total $n = 34$), as were all Mendelian incompatible genotypes within families.

DNA samples in Sample 2 were typed for 4,310,364 markers on the Illumina HumanOmni5 Beadchip, version 1.0. Genotypes were called using Illumina GenomeStudio. Analysis was restricted to the region of chromosome 2 genotyped for Sample 1. Samples were required to have call rate = 0.98, and samples with 10th percentile of GenCall scores < 0.42 over all markers passing initial QC (call rate = 0.90, $p > 10^{-6}$ for deviation from HWP) were subject to manual inspection of fluorescence intensity data (B allele frequency) plotted against map position of at least one autosome. Before analysis, markers were subject to a more stringent QC (call rate = 0.98, MAF = 0.01). Genetic sex was verified by means of X-chromosome heterozygosity and percentage of successfully called Y-chromosome genotypes. Relationships and unintentional (non-)duplicates were checked by means of PLINK's --genome function⁴⁴ applied to a sparse set (pairwise $r^2 < 0.1$ between markers) of common polymorphisms (MAF = 0.05). Unreported relationships more distant than second-degree were classified as unrelated.

We augmented the fine-mapping marker panel for Sample 1 by imputation⁴⁵. Because none of the 1000 Genomes Phase 3 populations is representative of our Ugandan genomes, we used a set of Ugandan genomes typed for the HumanOmni5 panel, including Sample 2 as a subset, as a reference for imputation. Haplotypes of 44,542 common variants (MAF \geq 0.5%) spanning the fine-mapping region \pm 500kb were determined by means of SHAPEIT2⁴⁶, including the available parent-offspring duos and trios for more accurate phasing. Haplotypes from a subset of 302 unrelated individuals from the HumanOmni5-genotyped sample composed the reference data set for imputation into the discovery cohort ($n = 892$, including some without a PTST- phenotype). Genotypes from the Sample 1 fine-mapping panel were prephased using SHAPEIT2 before imputation in 5-Mb segments with 500 kb overlap using IMPUTE2⁴⁵. Imputation yielded an augmented panel of 40,335 SNPs with IMPUTE2 imputation quality score⁴⁷ \geq 0.5.

We carried out a principal components analysis (PCA) on the 471 Sample 2 individuals passing QC to detect ancestry outliers and to correct for population structure during association analysis (see below). A genome-wide panel of 160,884 common (MAF \geq 0.05) independent (pairwise $r^2 < 0.1$) variants passing marker QC from the HumanOmni5 panel was chosen, excluding four genomic regions with extensive linkage disequilibrium, which can create artifactual principal components (PCs)⁴⁸: Chr. 2, 135–137 megabasepairs (Mb) (lactase gene *LCT*), Chr. 6, 27–35 Mb (HLA region), Chr. 8, 6–16 Mb (inversion polymorphism), and Chr. 17, 40–45 Mb (extensive LD in admixed populations). We calculated principal components (PCs) by two different methods: first, using EIGENSOFT⁴⁹, which assumes that all individuals are unrelated; and second, using PCAiR⁵⁰, which performs PCA on an optimal unrelated subset of the sample and which uses genotype loadings to project PCs for relatives. Although the PCAiR approach is more valid for family data, we used EIGENSOFT PCs in association analyses because they resulted in a smaller genomic control (GC) parameter value (see below). To confirm African ancestry, a second PCA was conducted with addition of 119 unrelated individuals from the HapMap CEU, YRI, CHB and JPT samples, using a panel of 130,718 markers in common between the Omni5 PCA panel described above and the 1000 Genomes Phase 1, version 3 data set.

Statistical methods

Association analysis on the imputed Sample 1 genotype data was conducted by means of logistic regression, using the generalized estimating equations (GEE) model implemented in the gee package in R to allow for correlations within families. The number of minor alleles from genotyped markers, or the allele dosage data (expected number of minor alleles) from imputation, were used as a genotype predictor under an additive model (on the logarithmic scale). The “exchangeable” correlation structure was specified, in which all relatives within a family were assumed equally correlated; if this model failed to converge to a stable estimate, the “independence” structure was used, which provides a still valid, albeit less powerful, approach. For this study, because of the limited sample size and the complexity of the statistical model, families were defined by grouping individuals connected by first-degree relationships; within-household correlations owing to common household environment, and correlations between more distant family members, were not modeled. Only imputed SNPs with MAF \geq 0.03 were tested for association, after it was discovered

that the GEE algorithm had difficulty converging with some of the rarer imputed variants, even under the “independence” correlation structure, whereas models on genotyped SNPs with MAF > 0.01 converged well. We chose GEE for association analysis, instead of a generalized linear mixed model (GLMM) adjusting for all relationships, not only because of model complexity but also because there were very few second- and third-degree relative pairs in either sample, and because complex correlations due to sharing the same household, the same bed, etc., are difficult to model by GLMM but are estimated from the data by GEE. With only a regional marker map, we were unable to assess inflation of test statistics by means of the genomic control parameter λ ⁵¹. However, the value of λ over the region of linkage was only 1.007, and the quantile-quantile plot of the results is consistent with no genome-wide inflation (see Results). Because we expect this region to harbor truly associated variants, we are confident that the type I error was well controlled. Following Sobota et al.⁵², we estimated the number of effective independent tests by isolating a set of low-dependence markers, using PLINK’s --indep-pairwise function with an r^2 threshold of 0.2. This approach yielded 6,246 effective independent tests for a nominal p value threshold of 8.0×10^{-6} for regionwide significance of 0.05; and for the Omni5 marker set, 6,103 independent tests for nominal $p = 8.1 \times 10^{-6}$.

Association analysis on Sample 2 was carried out in similar fashion, except that the fourth PC from the EIGENSOFT PCA was included as a predictor to adjust for population structure. The first 20 PCs were evaluated for association with the PTST– phenotype in Sample 2. PCs 3 and 4 were found to be significant when included singly, but in the presence of PC 4, PC 3 had a nonsignificant effect, and thus only PC4 was included in association analysis as a covariate. A sparse genome-wide scan of about 10,000 SNPs from the Sample 2 Omni5 panel, excluding regions implicated in TB susceptibility (the HLA region, but also all genes mentioned in two previous reports^{28, 53}) was conducted to obtain an estimate of the genomic control (GC) parameter λ for genome-wide inflation of test statistics⁵¹. Because λ from the final analysis was greater than 1.05, we corrected association p values for genome-wide inflation by the method of Bacanu et al.⁵⁴. It was uncertain what was causing the overall inflation of test statistics. One possibility was that inflation was caused by including markers with low minor allele counts, but the value of λ was not reduced by increasing the minimum MAF to several values from 0.03 to 0.10. Second, we compared λ from association analyses adjusting for PC 4 from EIGENSOFT, and adjusting for four PCs from PCAiR that were significantly associated with PTST–, and found that adjusting for EIGENSOFT PC4 resulted in a smaller value of λ ⁵⁴.

We conducted meta-analysis by the inverse-variance-weighted fixed-effect method, and calculated Cochran’s Q statistic and I^2 to assess effect heterogeneity between the two samples, using a custom script for the statistical software R.

Haplotypes of 13 SNPs in genes *GTDC1* and *ZEB2* were determined for both Samples 1 and 2 by means of SHAPEIT2, with the --duohmm option to make use of parent/child relationships. Haplotypes from two sets of SNPs, a set of 11 and a set of two, showing linkage disequilibrium were used for haplotype-based association analysis. Best-guess haplotypes from these two sets were counted, and haplotypes with sample frequencies between 3% and 20% were tested for association with PTST– vs. all other pooled

haplotypes, under the same GEE regression model used for single-marker association testing.

We used the restricted maximum likelihood (REML) estimation approach in the GCTA software package⁵⁵ to partition genetic variance in Sample 2 explained by the specific region on Chr. 2 (position 117,911,357 to 168,853,091) and, separately, all other genotyped SNPs across the genome. Briefly, we filtered SNPs (excluding SNPs with call rate < 0.95 and minor allele frequency < 0.05), generated separate genetic relationship matrices for the region on Chr. 2 and the rest of the genome, then performed REML estimation using the expectation maximization fitting method to estimate the proportion of “risk” for being PTST explained by each of the two genetic partitions (i.e., region on Chr. 2 & all other SNPs). REML analysis was adjusted for age, sex, and HIV status.

Differences in proportions in body-mass wasting between PTST– and non-PTST– subsets in the sample measured for body mass composition were evaluated by Fisher’s exact test.

Annotating strongly associated variants

We explored the likely effects of genetic variants with the most significant association results with information from several well-known databases. We obtained Combined Annotation-dependent Depletion (CADD) scores⁵⁶, a measure of deleteriousness based on evolutionary conservation and on numerous measures of regulatory importance and predicted protein effects, from the CADD Web site (<http://cadd.gs.washington.edu/>). We report CADD scores as PHRED-like scores, in which a score of 10x indicates pathogenicity within the top 100×10^{-x} percent of possible variants genome-wide. We extracted specific information on chromatin structure, effects on DNA regulatory motifs and association results from other GWAS and expression quantitative trait locus (eQTL) studies from the HaploReg v4.1⁵⁷ Web site (<http://archive.broadinstitute.org/mammals/haploreg/haploreg.php>), specifying the ChromHMM (Core 15-state model) algorithm for chromatin structure determination. We searched the GTEx database⁵⁸ for prominent PTST– associated markers for evidence of eQTL activity in 53 human tissues. Finally, we acquired a measure of overall evidence for a regulatory role from RegulomeDB (⁵⁹; <http://www.regulomedb.org/>).

Supplementary Material

Refer to Web version on PubMed Central for supplementary material.

Acknowledgments

The authors wish to acknowledge the contributions made by senior physicians, medical officers, health visitors, laboratory and data personnel: Dr. Lorna Nshuti, Dr. Roy Mugerwa, Dr. Alphonse Okwera, Dr. Deo Mulindwa, Dr. Christopher Whalen, Denise Johnson, Allan Chiunda, Mark Breda, Dennis Dobbs, Mary Rutaro, Albert Muganda, Richard Bamuhimbisa, Yusuf Mulumba, Deborah Nsamba, Barbara Kyeyune, Faith Kintu, Gladys Mpalanyi, Janet Mukose, Grace Tumusiime, Pierre Peters, Annet Kawuma, Saidah Menya, Joan Nassuna, Keith Chervenak, Karen Morgan, Alfred Etwom, Micheal Angel Mugerwa, and Lisa Kucharski. We would like to acknowledge Dr. Francis Adatu Engwau, former Head of the Uganda National Tuberculosis and Leprosy Program, for supporting this project. We would like to acknowledge the medical officers, nurses and counselors at the National Tuberculosis Treatment Centre, Mulago Hospital, the Ugandan National Tuberculosis and Leprosy Program and the Uganda Tuberculosis Investigation Bacteriological Unit, Wandegaya, for their contributions to this study. Clinical study implementation and data management were supported by the National Institutes of Health, grants N01-AI95383, HHSN266200700022C/N01-AI70022. Genotyping and data analysis was supported by R01HL096811 and analyses

were also supported by T32HL007567. This study would not be possible without the generous participation of the Ugandan patients and families.

References

1. World Health Organization. Global Tuberculosis Report. WHO Press; Geneva, Switzerland: 2016.
2. Comstock GW. Epidemiology of tuberculosis. *Am Rev Respir Dis.* 1982; 125:8–15. [PubMed: 7073104]
3. Stein CM, Sausville L, Wejse C, Sobota RS, Zetola NM, Hill PC, et al. Genomics of human pulmonary tuberculosis: from genes to pathways. *Curr Genet Med Reports.* 2017; 5:149–166.
4. Möller M, Hoal EG. Current findings, challenges and novel approaches in human genetic susceptibility to tuberculosis. *Tuberculosis (Edinb).* 2010; 90:71–83. [PubMed: 20206579]
5. Cooke GS, Campbell SJ, Bennett S, Lienhardt C, McAdam KP, Sirugo G, et al. Mapping of a novel susceptibility locus suggests a role for *MC3R* and *CTSZ* in human tuberculosis. *Am J Respir Crit Care Med.* 2008; 178:203–207. [PubMed: 18420963]
6. Bellamy R. Genetics and pulmonary medicine: 3. Genetic susceptibility to tuberculosis in human populations. *Thorax.* 1998; 53:588–593. [PubMed: 9797760]
7. Stein CM, Zalwango S, Malone LL, Won S, Mayanja-Kizza H, Mugerwa RD, et al. Genome scan of *M. tuberculosis* infection and disease in Ugandans. *PLoS ONE.* 2008; 3:e4094. [PubMed: 19116662]
8. Mahasirimongkol S, Yanai H, Nishida N, Ridruechai C, Matsushita I, Ohashi J, et al. Genome-wide SNP-based linkage analysis of tuberculosis in Thais. *Genes Immun.* 2009; 10:77–83. [PubMed: 18843276]
9. Miller EN, Jamieson SE, Joberty C, Fakiola M, Hudson D, Peacock CS, et al. Genome-wide scans for leprosy and tuberculosis susceptibility genes in Brazilians. *Genes Immun.* 2004; 5:63–67. [PubMed: 14735151]
10. Thye T, Vannberg FO, Wong SH, Owusu-Dabo E, Osei I, Gyapong J, et al. Genome-wide association analyses identifies a susceptibility locus for tuberculosis on chromosome 18q11.2. *Nat Genet.* 2010; 42:739–741. [PubMed: 20694014]
11. Thye T, Owusu-Dabo E, Vannberg FO, van Crevel R, Curtis J, Sahiratmadja E, et al. Common variants at 11p13 are associated with susceptibility to tuberculosis. *Nat Genet.* 2012; 44:257–259. [PubMed: 22306650]
12. Chimusa ER, Zaitlen N, Daya M, Möller M, van Helden PD, Mulder NJ, et al. Genome-wide association study of ancestry-specific TB risk in the South African Coloured population. *Hum Mol Genet.* 2014; 23:796–809. [PubMed: 24057671]
13. Curtis J, Luo Y, Zenner HL, Cuchet-Lourenço D, Wu C, Lo K, et al. Susceptibility to tuberculosis is associated with variants in the *ASAP1* gene encoding a regulator of dendritic cell migration. *Nat Genet.* 2015; 47:523–527. [PubMed: 25774636]
14. Mahasirimongkol S, Yanai H, Mushiroda T, Promphittayart W, Wattanapokayakit S, Phromjai J, et al. Genome-wide association studies of tuberculosis in Asians identify distinct at-risk locus for young tuberculosis. *J Hum Genet.* 2012; 57:363–367. [PubMed: 22551897]
15. Png E, Alisjahbana B, Sahiratmadja E, Marzuki S, Nelwan R, Balabanova Y, et al. A genomewide association study of pulmonary tuberculosis susceptibility in Indonesians. *BMC Med Genet.* 2012; 13:5. [PubMed: 22239941]
16. Sobota RS, Stein CM, Kodaman N, Scheinfeldt LB, Maro I, Wieland-Alter W, et al. A locus at 5q33.3 confers resistance to tuberculosis in highly susceptible individuals. *Am J Hum Genet.* 2016; 98:514–524. [PubMed: 26942285]
17. Cobat A, Poirier C, Hoal E, Boland-Auge A, de La Rocque F, Corrad F, et al. Tuberculin skin test negativity is under tight genetic control of chromosomal region 11p14–15 in settings with different tuberculosis endemicities. *J Inf Dis.* 2015; 211:317–321. [PubMed: 25143445]
18. Stein CM. Genetic epidemiology of tuberculosis susceptibility: impact of study design. *PLoS Pathog.* 2011; 7:e1001189. [PubMed: 21283783]

19. Cobat A, Gallant CJ, Simkin L, Black GF, Stanley K, Hughes J, et al. Two loci control tuberculin skin test reactivity in an area hyperendemic for tuberculosis. *J Exp Med*. 2009; 206:2583–2591. [PubMed: 19901083]
20. Cobat A, Barrera LF, Henao H, Arbeláez P, Abel L, García LF, et al. Tuberculin skin test reactivity is dependent on host genetic background in Colombian tuberculosis household contacts. *Clin Infect Dis*. 2012; 54:968–971. [PubMed: 22291100]
21. Sobota RS, Stein CM, Kodaman N, Maro I, Wieland-Alter W, Igo RP Jr, et al. A chromosome 5q31.1 locus associates with tuberculin skin test reactivity in HIV-positive individuals from tuberculosis hyper-endemic regions in east Africa. *PLoS Genet*. 2017; 13:e1006710. [PubMed: 28628665]
22. Stein CM, Hall NB, Malone LL, Mupere E. The household contact study design for genetic epidemiological studies of infectious diseases. *Front Genet*. 2013; 4:61. [PubMed: 23641253]
23. Stein CM, Zalwango S, Malone LL, Thiel BA, Mupere E, Nsereko M, et al. Resistance and susceptibility to *Mycobacterium tuberculosis* infection and disease in tuberculosis households in Kampala, Uganda. *Am J Epidemiol*. 2018; doi: 10.1093/aje/kwx380
24. Ma N, Zalwango S, Malone LL, Nsereko M, Wampande EM, Thiel BA, et al. Clinical and epidemiological characteristics of individuals resistant to *M. tuberculosis* infection in a longitudinal TB household contact study in Kampala, Uganda. *BMC Infect Dis*. 2014; 14:352. [PubMed: 24970328]
25. Simmons J, Stein CM, Seshadri C, Campo M, Alter G, Fortune S, et al. Immunologic mechanisms of human resistance to persistent *Mycobacterium tuberculosis* infection. *Nat Rev Immunol*. 2018
26. Hawn TR, Day TA, Scriba TJ, Hatherill M, Hanekom WA, Evans TG, et al. Tuberculosis vaccines and prevention of infection. *Microbiol Mol Biol Rev*. 2014; 78:650–671. [PubMed: 25428938]
27. Verrall AJ, Netea MG, Alisjahbana B, Hill PC, Van Crevel R. Early clearance of *Mycobacterium tuberculosis*: a new frontier in prevention. *Immunology*. 2014; 141:506–513. [PubMed: 24754048]
28. Hall NB, Igo RP Jr, Malone LL, Truitt B, Schnell A, Tao L, et al. Polymorphisms in *TICAM2* and *IL1B* are associated with TB. *Genes Immun*. 2015; 16:127–133. [PubMed: 25521228]
29. Guwatudde D, Nakakeeto M, Jones-Lopez EC, Maganda A, Chiunda A, Mugerwa RD, et al. Tuberculosis in household contacts of infections cases in Kampala, Uganda. *Am J Epidemiol*. 2003; 158:887–898. [PubMed: 14585767]
30. Mupere E, Malone L, Zalwango S, Okwera A, Nsereko M, Tisch DJ, et al. Wasting among Uganda men with pulmonary tuberculosis is associated with linear regain in lean tissue mass during and after treatment in contrast to women with wasting who regain fat tissue mass: prospective cohort study. *BMC Infect Dis*. 2014; 14:24. [PubMed: 24410970]
31. Mupere E, Malone L, Zalwango S, Chiunda A, Okwera A, Parraga I, et al. Lean tissue mass wasting is associated with increased risk of mortality among women with pulmonary tuberculosis in urban Uganda. *Ann Epidemiol*. 2012; 22:466–473. [PubMed: 22575813]
32. Mupere E, Zalwango S, Chiunda A, Okwera A, Mugerwa R, Whalen C. Body composition among HIV-seropositive and HIV-seronegative adult patients with pulmonary tuberculosis in Uganda. *Ann Epidemiol*. 2010; 30:210–216.
33. Mupere E, Parraga IM, Tisch DJ, Mayanja HK, Whalen CC. Low nutrient intake among adult women and patients with severe tuberculosis disease in Uganda: a cross-sectional study. *BMC Public Health*. 2012; 12:1050. [PubMed: 23217171]
34. Ezeamama AE, Mupere E, Oloya J, Martinez L, Kakaire R, Yin X, et al. Age, sex and nutritional status modify the CD4+ T-cell recovery rate in HIV-tuberculosis co-infected patients on combination antiretroviral therapy. *Int J Infect Dis*. 2015; 35:73–79. [PubMed: 25910854]
35. Aslibekyan S, Demerath EW, Mendelson M, Zhi D, Guan W, Liang L, et al. Epigenome-wide study identifies novel methylation loci associated with body mass index and waist circumference. *Obesity*. 2015; 23:1493–1501. [PubMed: 26110892]
36. Wu LM, Wang J, Conidi A, Zhao C, Wang H, Ford Z, et al. Zeb2 recruits HDAC-NuRD to inhibit Notch and controls Schwann cell differentiation and remyelination. *Nat Neurosci*. 2016; 19:1060–72. [PubMed: 27294509]

37. Seshadri C, Sedaghat N, Campo M, Peterson G, Wells RD, Olson GS, et al. Transcriptional networks are associated with resistance to *Mycobacterium tuberculosis* infection. *PLoS ONE*. 2017; 12:e0175844. [PubMed: 28414762]
38. Pérez-Guzmán C, Vargas MH. Hypcholesterolemia: A major risk factor for developing pulmonary tuberculosis? *Med Hypotheses*. 2006; 66:1227–1230. [PubMed: 16500037]
39. Han R, Kornfeld H, Martens G. Is hypercholesterolemia a friend or foe of tuberculosis? *Infect Immun*. 2009; 77:3514. [PubMed: 19617455]
40. Martens GW, Arikan MC, Lee J, Ren F, Vallerskog T, Kornfeld H. Hypercholesterolemia impairs immunity to tuberculosis. *Infect Immun*. 2008; 76:3464–3472. [PubMed: 18505807]
41. Martens GW, Vallerskog T, Kornfeld H. Hypercholesterolemic LDL receptor-deficient mice mount a neutrophilic response to tuberculosis despite the timely expression of protective immunity. *J Leukoc Biol*. 2012; 91:849–857. [PubMed: 22227965]
42. Parihar SP, Guler R, Khutlang R, Lang DM, Hurdayal R, Mhlanga MM, et al. Statin therapy reduces the mycobacterium tuberculosis burden in human macrophages and in mice by enhancing autophagy and phagosome maturation. *J Inf Dis*. 2014; 209:754–763. [PubMed: 24133190]
43. VanItallie TB, Yang MU, Heymsfield SB, Funk RC, Boileau RA. Height-normalized indices of the body's fat-free mass and fat mass: potentially useful indicators of nutritional status. *Am J Clin Nutr*. 1990; 52:953–959. [PubMed: 2239792]
44. Purcell S, Neale B, Todd-Brow K, Thomas L, Ferreira MAR, Bender D, et al. PLINK: a toolset for whole-genome association and population-based linkage analysis. *Am J Hum Genet*. 2007; 81:559–575. [PubMed: 17701901]
45. Howie BN, Donnelly P, Marchini J. A flexible and accurate genotype imputation method for the next generation of genomewide association studies. *PLoS Genet*. 2009; 5:e1000529. [PubMed: 19543373]
46. Delaneau O, Zagury J-F, Marchini J. Improved whole-chromosome phasing for disease and population genetic studies. *Nat Methods*. 2013; 10:5–6. [PubMed: 23269371]
47. Marchini J, Howie B. Genotype imputation for genome-wide association studies. *Nat Rev Genet*. 2010; 11:499–511. [PubMed: 20517342]
48. Novembre J, Johnson T, Bryc K, Kutalik Z, Boyko AR, Auton A, et al. Genes mirror geography within Europe. *Nature*. 2008; 456:98–101. [PubMed: 18758442]
49. Patterson N, Price AL, Reich D. Population structure and eigenanalysis. *PLoS Genet*. 2006; 2:e190. [PubMed: 17194218]
50. Conomos MP, Miller MB, Thornton TA. Robust inference of population structure for ancestry prediction and correction of stratification in the presence of relatedness. *Genet Epidemiol*. 2015; 39:276–293. [PubMed: 25810074]
51. Devlin B, Roeder K. Genomic control for association studies. *Biometrics*. 1999; 55:997–1004. [PubMed: 11315092]
52. Sobota RS, Shriner D, Kodaman N, Goodloe R, Zheng W, Gao Y-T, et al. Addressing population-specific multiple testing burdens in genetic association studies. *Ann Hum Genet*. 2015; 79:136–147. [PubMed: 25644736]
53. Stein, CM. *Encyclopedia of Life Sciences (eLS)*. John Wiley & Sons; Chichester: 2012. Genetics of susceptibility to tuberculosis.
54. Bacanu S-A, Devlin B, Roeder K. The power of genomic control. *Am J Hum Genet*. 2000; 66:1933–1944. [PubMed: 10801388]
55. Yang J, Lee SH, Goddard ME, Visscher PM. GCTA: a tool for genome-wide complex trait analysis. *Am J Hum Genet*. 2011; 88:76–82. [PubMed: 21167468]
56. Kircher M, Witten DM, Jain P, O'Roak BJ, Cooper GM, Shendure J. A general framework for estimating the relative pathogenicity of human genetic variants. *Nat Genet*. 2014; 46:310–315. [PubMed: 24487276]
57. Ward LD, Kellis M. HaploReg: a resource for exploring chromatin states, conservation and regulatory motif alterations within sets of genetically linked variants. *Nucleic Acids Res*. 2012; 40:D930–D934. [PubMed: 22064851]
58. GTEx Consortium. The Genotype-Tissue Expression (GTEx) project. *Nat Genet*. 2013; 45:580–585. [PubMed: 23715323]

59. Boyle AP, Hong EL, Hariharan M, Cheng Y, Schaub MA, Kasowski M, et al. Annotation of functional variation in personal genomes using RegulomeDB. *Genome Res.* 2012; 22:1790–1797. [PubMed: 22955989]

Author Manuscript

Author Manuscript

Author Manuscript

Author Manuscript

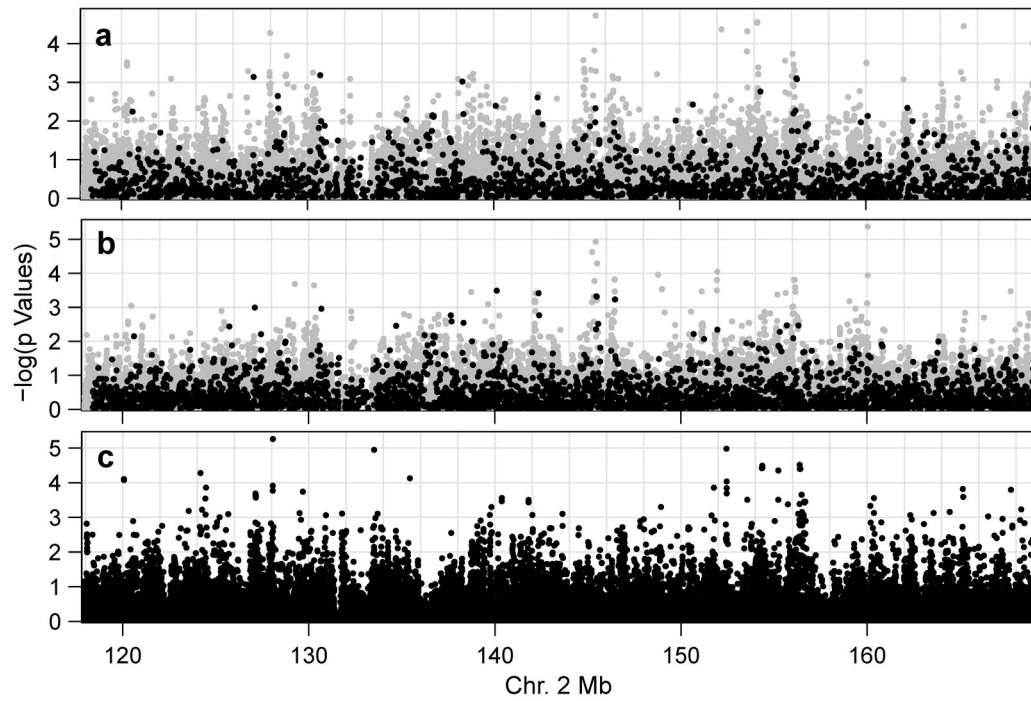


Figure 1. Manhattan plots of association results from (A) the meta-analysis, (B) Sample 1 and (C) Sample 2. Genotyped and imputed markers are represented as black and blue dots, respectively.

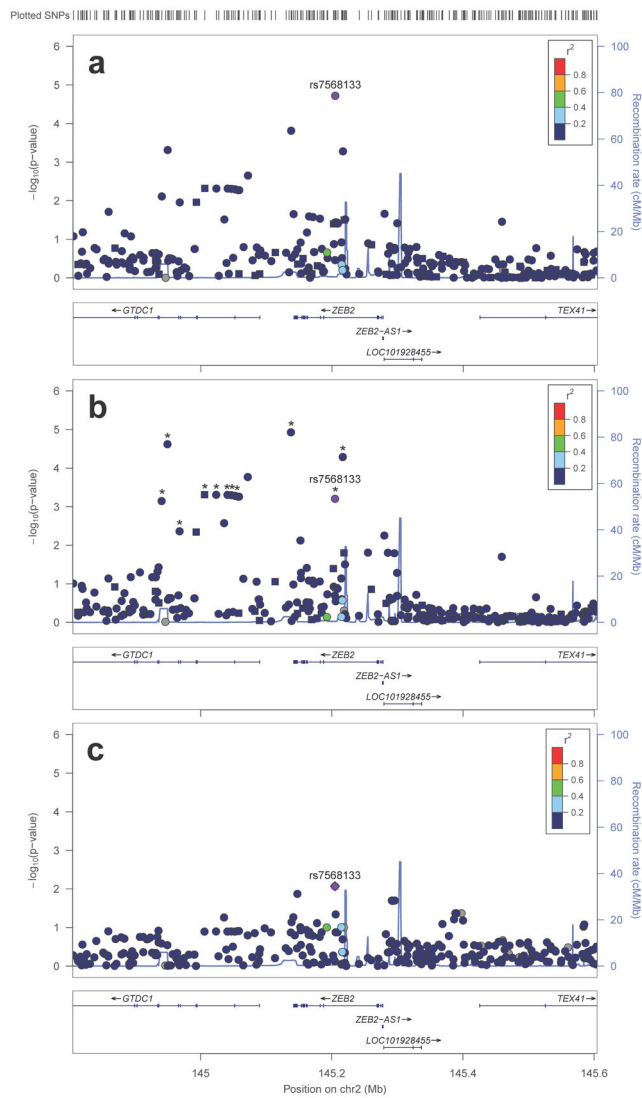


Figure 2. LocusZoom plots of the chromosome 2 region surrounding rs7568133, for (A) the meta-analysis, (B) Sample 1 only and (C) Sample 2 only. In A and B, genotyped and imputed markers are represented by squares and circles, respectively. In B, markers selected for haplotype-based analysis (see Online Resource 1, Supplementary Figure 2) are marked with asterisks. The LD structure shown is that of the 1000 Genomes 2014 AFR population.

Table 1

Characteristics of the two Ugandan PTST- samples.

	PTST-	Non-PTST-	Total	<i>p</i>
Sample 1				
<i>n</i>	81	666	747	—
Active TB	0 (0.0%)	165 (24.8%)	165 (22.1%)	—
Female	38 (46.9%)	276 (41.4%)	314 (42.0%)	0.41
Age, y	9.3 ± 8.8	17.8 ± 13.5	16.9 ± 13.3	< 0.001
HIV+	4 (5.4%)	80 (13.0%)	84 (12.2%)	0.061
Sample 2				
<i>n</i>	33	438	471	—
Active TB	0 (0.0%)	201 (45.9%)	201 (42.7%)	—
Female	16 (48.5%)	215 (49.1%)	231 (49.0%)	0.99
Age, y	11.5 ± 12.5	21.6 ± 13.4	20.9 ± 13.5	< 0.001
HIV+	3 (9.4%)	56 (12.9%)	59 (12.7%)	0.78

Values are presented either as *n* (% of total sample) or as mean ± SD. Non-PTST-, LTBI plus active TB; *p*, *p* value for test of differences between PTST- and non-PTST- individuals, by 2×2 χ^2 test for sex, Wilcoxon rank-sum test for age, and Fisher's exact test for HIV status.

Table 2

Most significant meta-analysis results.

Marker	Gene	Position	Alleles	Sample 1					Sample 2					Meta-analysis		
				RAF	Info	OR	95% CI	p	RAF	OR	95% CI	p	OR	95% CI	p	
rs2028211	<i>BN1</i>	127,901,657	C/A	0.1460	0.78	1.43	(0.80, 2.53)	0.22	0.1470	3.92	(2.18, 7.07)	5.4E-06	2.33	(1.55, 3.52)	5.3E-05	
rs7568133	<i>ZEB2</i>	145,204,976	A/G	0.4952	0.82	2.00	(1.35, 2.98)	0.00062	0.4775	2.55	(1.27, 5.11)	0.0085	2.12	(1.50, 3.00)	1.9E-05	
rs10169306	<i>AC023469.1</i>	151,926,472	A/G	0.0635	0.84	1.57	(0.84, 2.95)	0.16	0.0687	4.26	(2.24, 8.11)	1.0E-05	2.56	(1.63, 4.02)	4.3E-05	
rs58110523	<i>FMNL2</i>	153,292,235	C/T	0.0486	0.84	2.85	(1.43, 5.66)	0.0028	0.0483	3.71	(1.48, 9.29)	0.0052	3.13	(1.80, 5.42)	4.8E-05	
rs74762979	<i>ARL6IP6</i>	153,804,898	G/A	0.0957	0.88	1.88	(1.07, 3.31)	0.028	0.0763	5.25	(2.39, 11.55)	3.7E-05	2.66	(1.68, 4.22)	2.9E-05	
rs114101795	<i>ARL6IP6</i>	153,825,388	A/G	0.0957	0.88	1.88	(1.07, 3.30)	0.028	0.0787	5.46	(2.45, 12.13)	3.2E-05	2.68	(1.69, 4.25)	2.8E-05	
rs79513402	<i>ARL6IP6</i>	153,829,134	C/T	0.0957	0.88	1.88	(1.07, 3.30)	0.029	0.0774	5.29	(2.40, 11.66)	3.6E-05	2.66	(1.68, 4.22)	2.9E-05	
rs78089492	<i>AC092684.1</i>	164,826,751	G/A	0.0737	0.92	2.54	(1.43, 4.52)	0.0015	0.0655	2.56	(1.27, 5.15)	0.0082	2.55	(1.64, 3.98)	3.6E-05	

Gene, gene that contains or is nearest to marker; Alleles, effect/other allele, where the reference is the minor allele in the sample; RAF, reference allele frequency; Info, IMPUTE2 information quality score.

Table 3

Body mass wasting in PTST– and non-PTST– Ugandan individuals.

	PTST–	Non-PTST–	<i>p</i>
BMI	6 (12.2%)	322 (21.0%)	0.14
Lean mass	2 (5.1%)	218 (17.9%)	<i>0.039</i>
Fat mass	8 (20.0%)	301 (24.6%)	0.51

Criteria for wasting were body-mass index (BMI) < 18.5 kg/m², fat mass index < 1.8 kg/m² for men and < 3.9 kg/m² for women, and lean mass index < 16.7 kg/m² for men and < 14.6 kg/m² for women³⁰. All tested participants were HIV-negative aged 15 years or older. Values are shown as *N*(%). *p*, *p* value by Fisher's exact test; values below 0.05 are *italicized*.